



Interstellar Prisms: Unlocking Small Scale Dispersion Measure Variations in Pulsars

Daniel Baker

Academia Sinica Institute of Astronomy and Astrophysics (ASIAA), No. 1, Sec. 4, Roosevelt Rd., Taipei 10617, Taiwan



Pulsars and Dispersion Measure

Regular, short period radio pulses are excellent probes for studying a wide range of exciting astrophysical phenomena from gravitational effects such as the Shapiro delay and gravitational waves to plasma physics in the Interstellar Medium (ISM). Fortunately, nature as seen fit to give us reliable sources of just that in the form of pulsars.

Rapidly rotating neutron stars emit beams of radiation from near their magnetic poles which, as the star rotates, may sweep past the Earth resulting in a pulse of radiation. The short duration of these pulses, combined with the extreme stability of the star's rotation, allows the arrival times of the pulses to be accurately predicted and measured. In turn, this allows us to detect any effects, such as those listed above, that change the arrival time of the pulses.

One of the most important of these effects is the dispersive effect of the ISM that results in the delayed arrival (t_{arr}) of the pulse at lower frequencies according to

$$t_{arr}(\nu) = t_{ref} + DM \left(\frac{1}{\nu^2} - \frac{1}{\nu_{ref}^2} \right)$$

for frequency ν compared to some reference arrival time t_{ref} and frequency ν_{ref} . The dispersion measure (DM) in this equation is the integrated electron density along the line of sight and K is a constant.

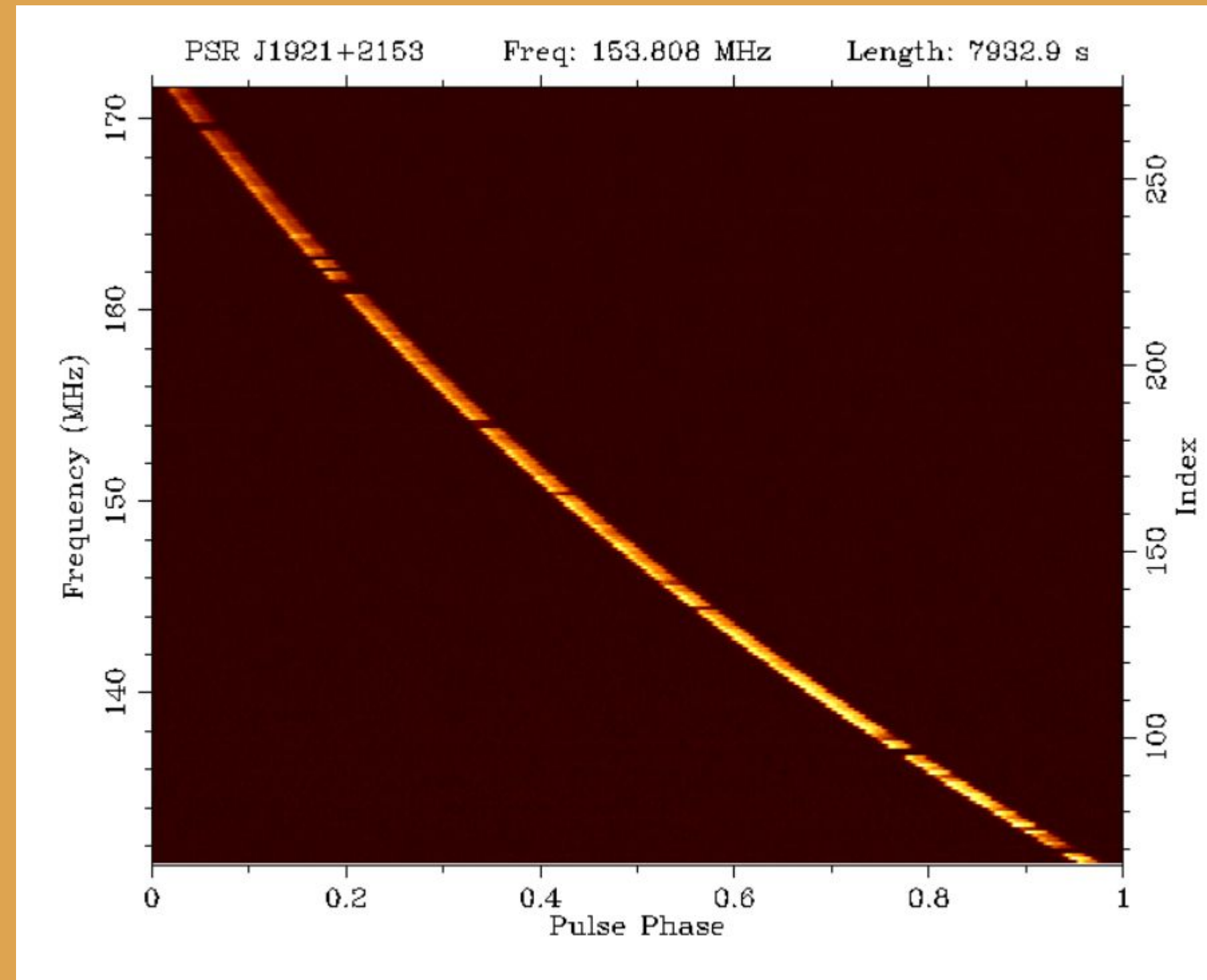


Figure 1: Dispersed profile of PSR J1921+2153 taken at LOFAR and averaged over several thousand pulses. From the thesis of Abubakr Ibrahim at <https://open.uct.ac.za/server/api/core/bitstreams/7e3414b9-20c0-4a19-8a58-88f160850c0/content>

Since DM is determined by the total electron column towards the pulsar, probing many pulsars is an excellent way to study the electron distribution in the Milky Way. Several galactic models have been built on the backs of these pulsar DM measurements including TC93 (Taylor & Cordes 1993), NE2001 (Cordes & Lazio 2003), and YMC16 (Yao et al. 2017).

However, since the DM is dependant on the sightline, it can also vary over time for an individual pulsar due to its motion or the motion of the Earth around the sun. This variation is an important nuisance parameter for experiments that rely on precise timing of pulsars such as pulsar timing arrays (PTAs) searching for gravitational wave signals. These observations are frequently taken at high frequencies to avoid other effects of the ISM, which can also make it difficult to detect changes in the DM without additional measurements at widely separated frequencies to detect the variation. Monitoring and modelling of the DMs near PTA pulsars is an important part of mitigating this effect.

Typically, this is done through high cadence measurements over a wide fractional bandwidth and the resulting DM time series is fit to a model including the changing ISM term and annual variation from the solar wind as shown below.

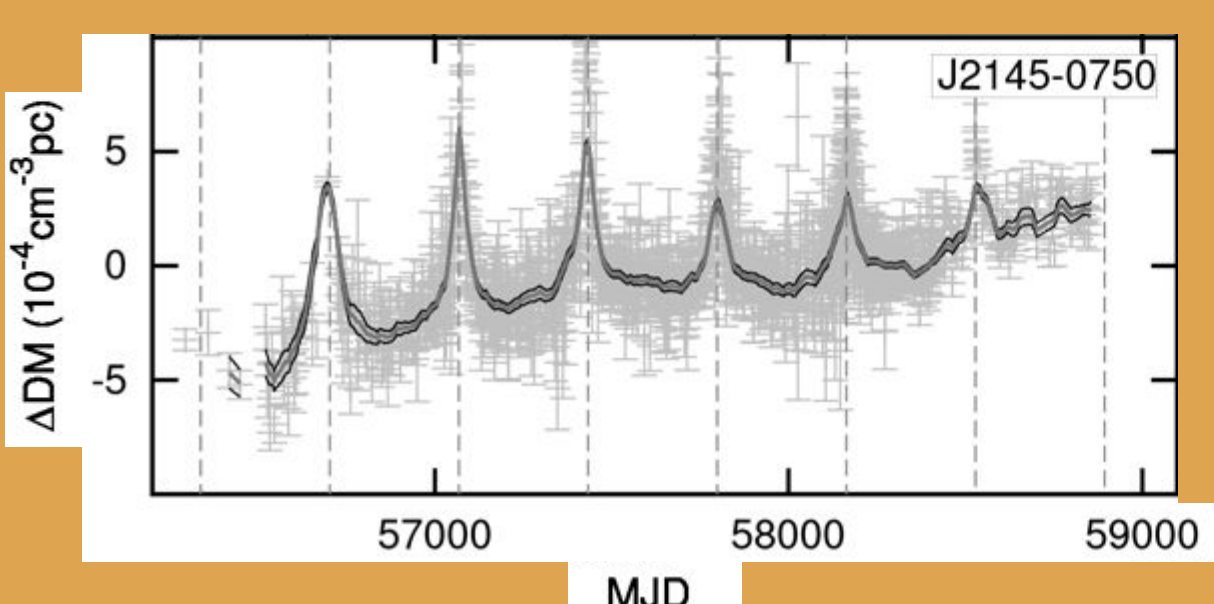


Figure 2: DM time series for J2145-0750 taken at LOFAR. Annual spike from where the line of sight passes near the sun as well as an overall gradient are visible. Figure cropped from Donner et al. 2020 <https://doi.org/10.1051/0004-6361/202039517>

ISM Scattering and Multiple Sightlines

In addition to the dispersive effects, the ISM also scatters the pulse as it propagates. Variations in the electron density cause the refractive index to vary, which distorts the wavefront and can cause multiple images of the pulsar to form. In the case of pulsars, much of this scattering seems to be dominated by a few thin screens along the line of sight, with images tending to form along a single straight line.

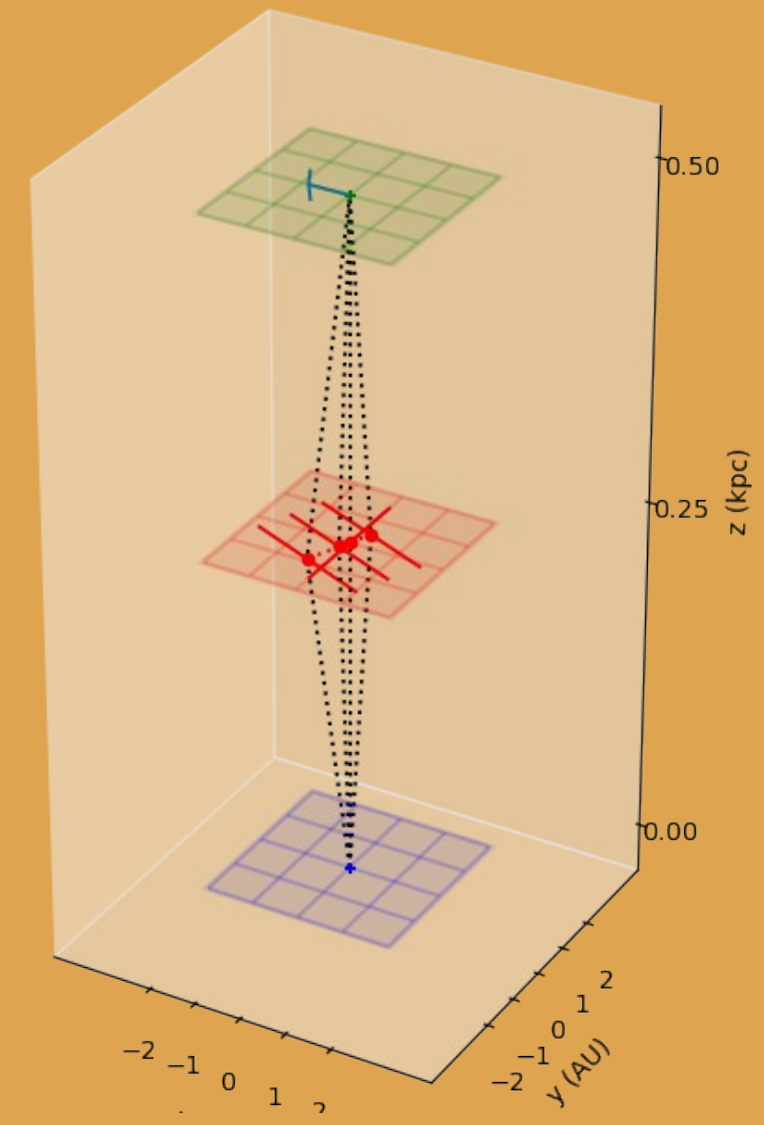


Figure 3: Simple schematic of a single thin scintillation screen. The signal travels from the pulsar (green) to the screen (red), where four scattering points are marked, before traveling to Earth (blue) where the signals are recombined.

When observed from Earth, these images interfere with each other and result in intensity modulations over time and frequency known as the dynamic spectrum. The linear nature of the images is evident in the Fourier transform of the dynamic spectrum known as the conjugate spectrum, with features positioned according to the relative time delays and Doppler shifts of pairs of images. These points lie along a series of inverted parabolas whose apexes lie along a single forward parabola with the same arc. This is a natural consequence of linear images whose geometric time delays can be shown to be proportional to the square of their angular offset and whose Doppler shifts are simple proportional. Working from these points it is possible to reconstruct the conjugate wavefield of the interference pattern which has points indicating the time delay and doppler shifts of each individual image.

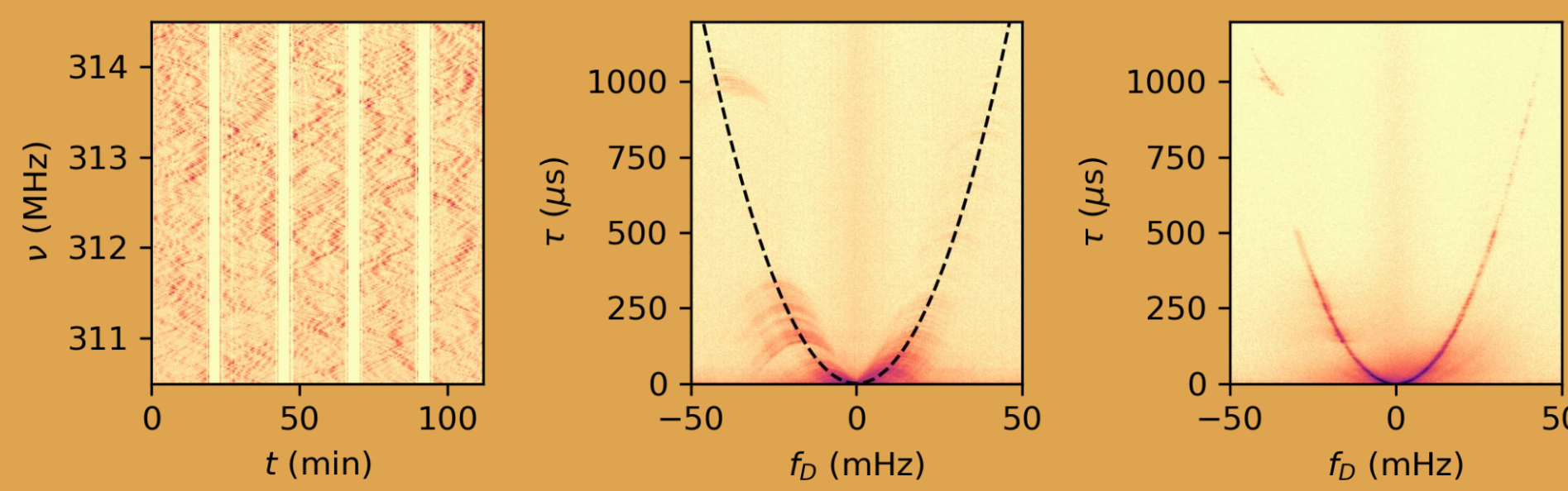


Figure 4: Example Dynamic Spectrum (left), Conjugate Spectrum (center), and Conjugate Wavefield (right) for observation of B0834-06 using Arecibo. The signature parabolic structure of a linear screen is clearly seen.

Since each image passes through a different point in the ISM, the question becomes: can we measure DM variation between images to probe the ISM on small scales.

The observation shown above, and used through the following sections, was taken on the Arecibo telescope on November 12 2005 as part of a VLBI campaign. It consists of four 8 MHz subbands of 32768 channels from 310.5 to 342.5 MHz with 1.25s integrations spanning nearly 2 hours by Brisken et al (DOI:[10.1088/0004-637X/708/1/232](https://doi.org/10.1088/0004-637X/708/1/232))

Tracking Individual Images

For the observation shown above, individual images become clearly isolated and so we can divide the observation into several subbands (in this case 8 spanning the full 32MHz). For a sequence of images we can fit a gaussian around the image at each frequency and fit for a DM using the evolution of the time delay of the peak.

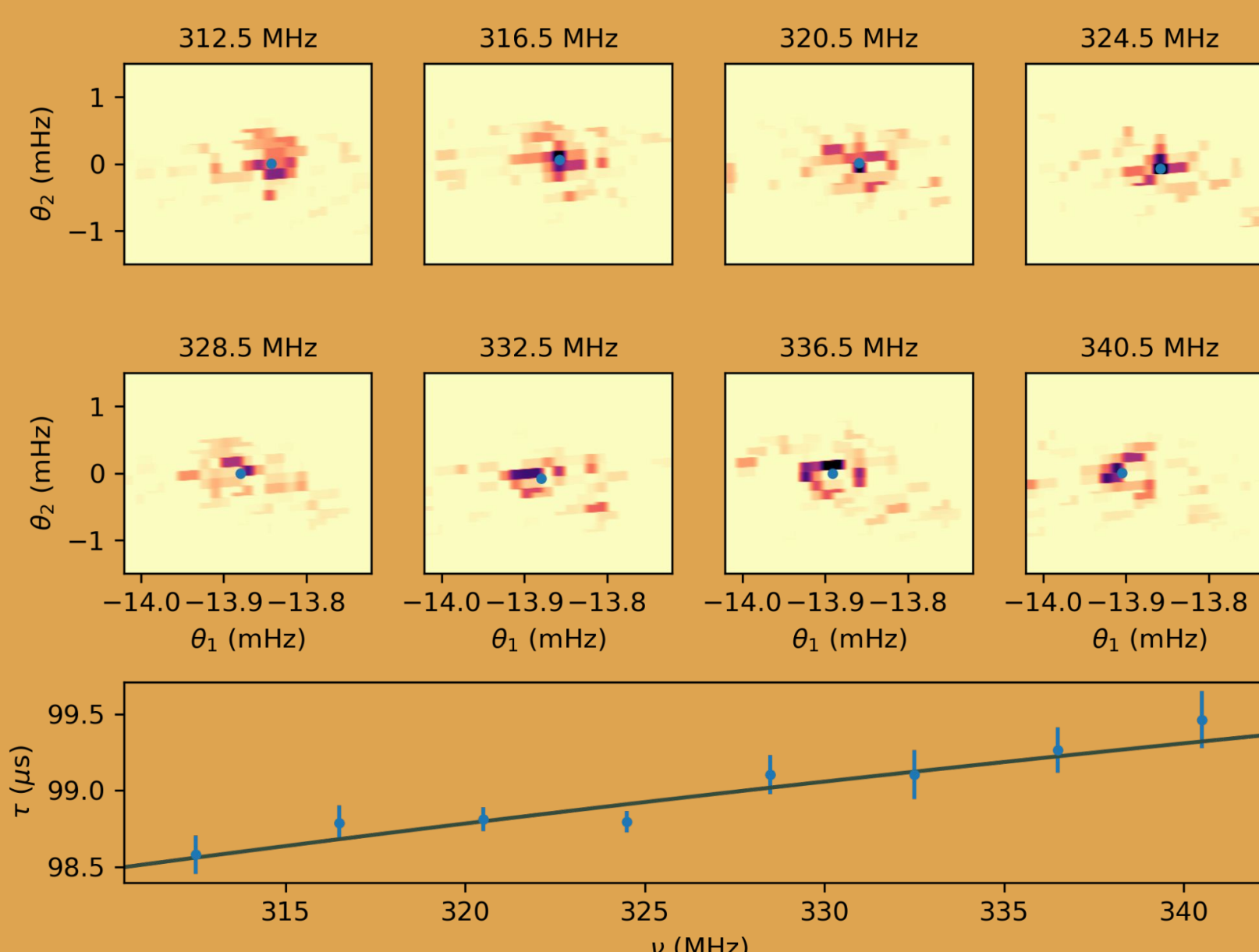


Figure 5: The position of a single image over several frequency channels (panels) and the best fit time delay (bottom). Note that the panels have been transformed into a space where the arc is a straight line for ease of identification.

Plotting DM against Doppler shift (which is linear in sky offset), we see a clear gradient across the arc of $6.5 \pm 0.6 \times 10^{-6} \text{ pc cm}^{-3} \text{ MHz}^{-1}$.

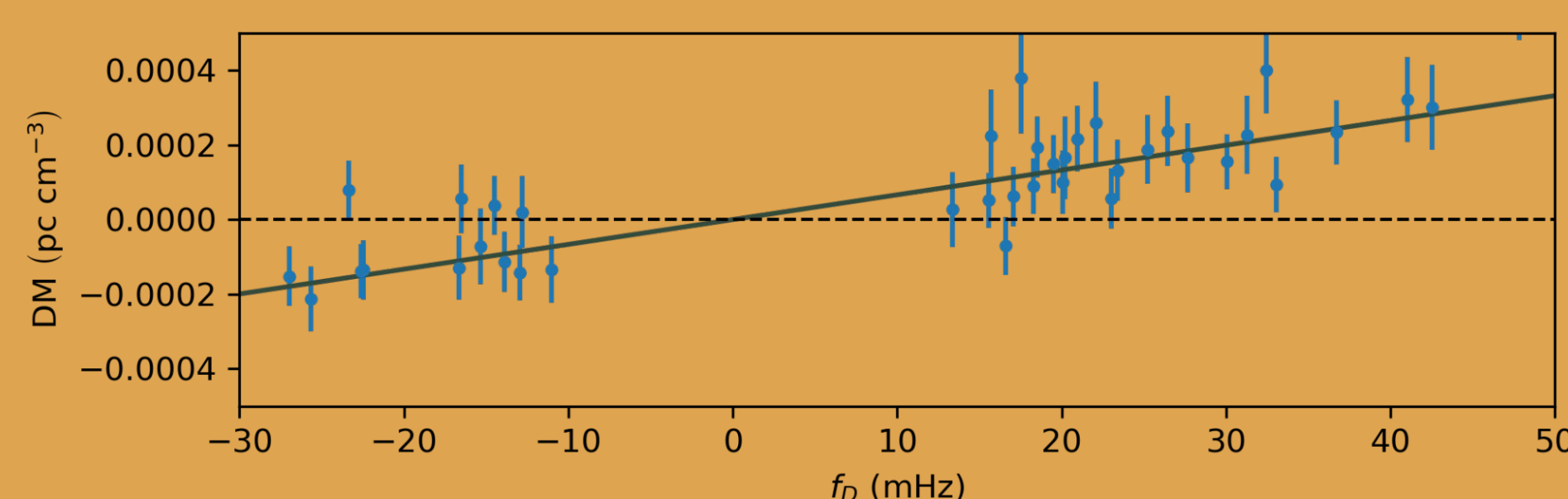


Figure 6: Dispersion measure as a function of image position shows a clear gradient across the arc.

Arc Correlations

Since not all observations have clear isolated features along the main arc, we would like to search for an additional approach using the arc as a whole. One possibility would be to take the arc in the lowest subband and correlate it against the arcs in the higher bands for each Doppler delay. For ease of visibility, we take the slightly different route of taking a series of values for the DM gradient and shifting each Doppler delay by the corresponding amount

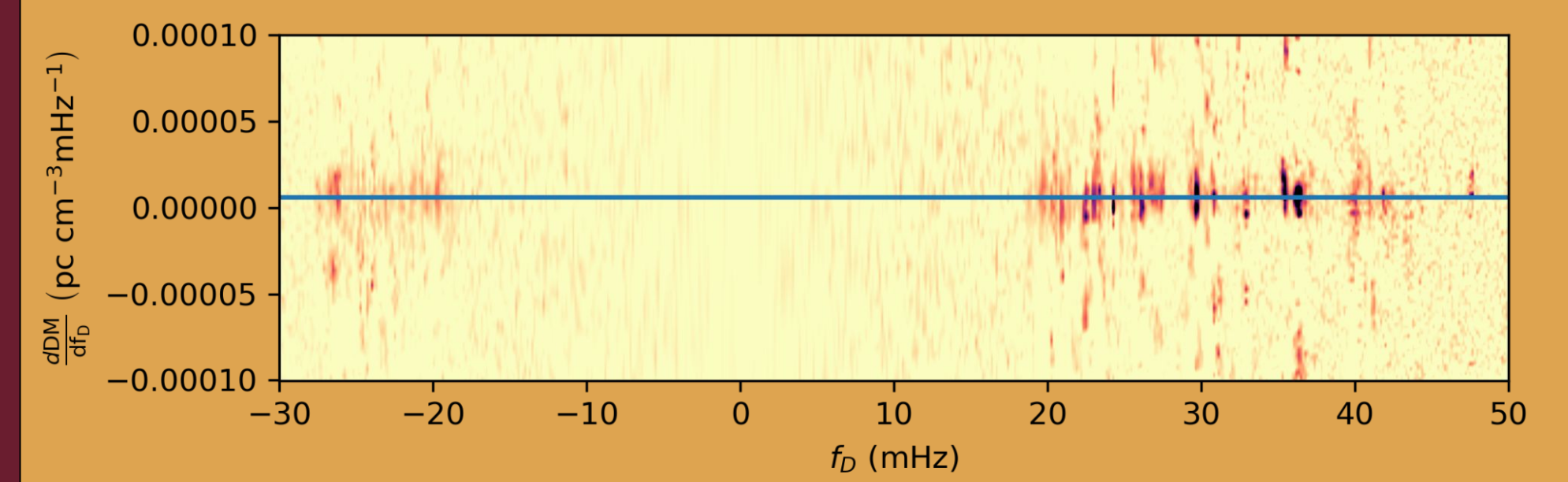


Figure 7: Example correlation as a function of DM gradient for all f_D points along the main arc for single band with a blue line indicating our best fit value from the image tracking method. The gap near 0 Doppler is caused by masking out small delays where the recovery is fuzzier.

Averaging over all bands gives a clear peak at $7.1 \pm 0.8 \times 10^{-6} \text{ pc cm}^{-3} \text{ MHz}^{-1}$

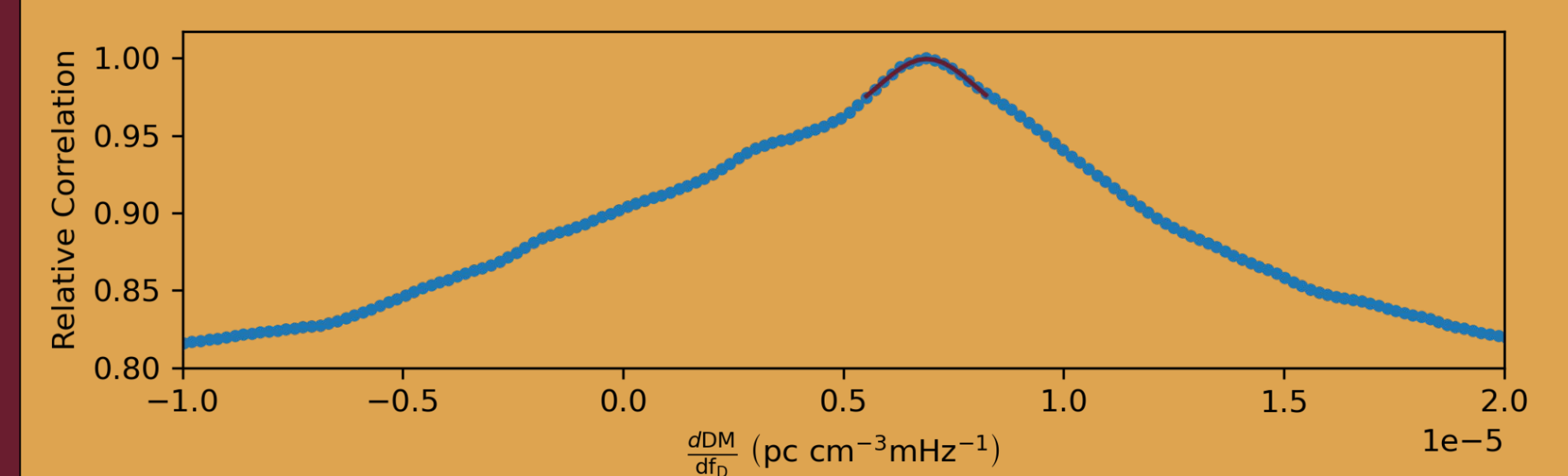


Figure 8: Normalized average correlation over Doppler shift. The peak at $7.1 \pm 0.8 \times 10^{-6} \text{ pc cm}^{-3} \text{ MHz}^{-1}$ is marked.

Additional Observations and Evolution

In addition to the observation shown previously, we also consider a series of observations also taken at Arecibo around the same time. These observations were taken at approximately weekly cadence with using several disjoint subbands. For this work we focus on the evolution between 317 and 335 MHz. These observations lacked the resolution to get the more distant portions of the parabola where individual images are easier to track, and so we focus on the correlation method.

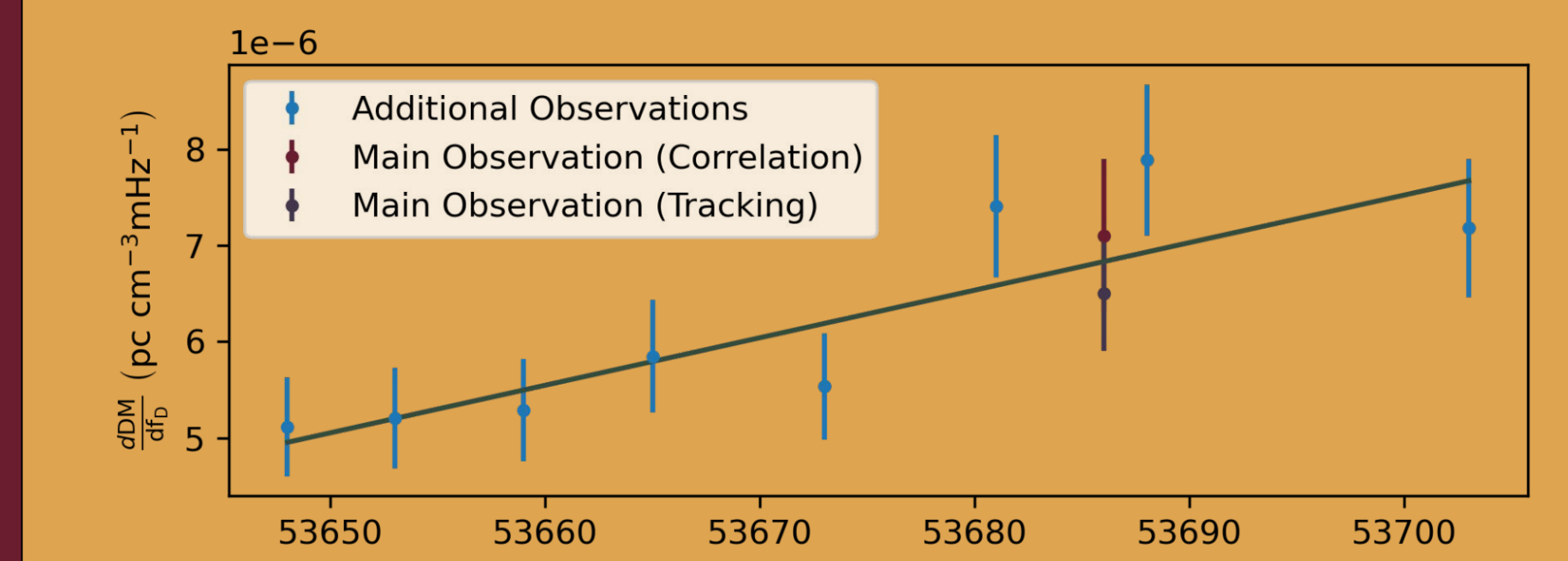


Figure 9: DM Gradient measurements over several weeks (blue) and measurements from the primary dataset using correlations (magenta) and feature tracking (purple). The green line shows the best linear fit to the correlation based measurements with a slope of $5 \pm 1 \times 10^{-6} \text{ pc cm}^{-3} \text{ MHz}^{-1} \text{ day}^{-1}$

Since a DM gradient causes the wavefront of the pulse to distort, the second derivative of the DM results in an apparent motion of the pulsar across the sky. In this case, the pulse would appear to shift along the line of images by $0.32 \pm 0.09 \text{ mas yr}^{-1}$. It is worth noting that since we only measure gradients along the screen, this represents a lower bound on the DM induced apparent motion of the pulsar.

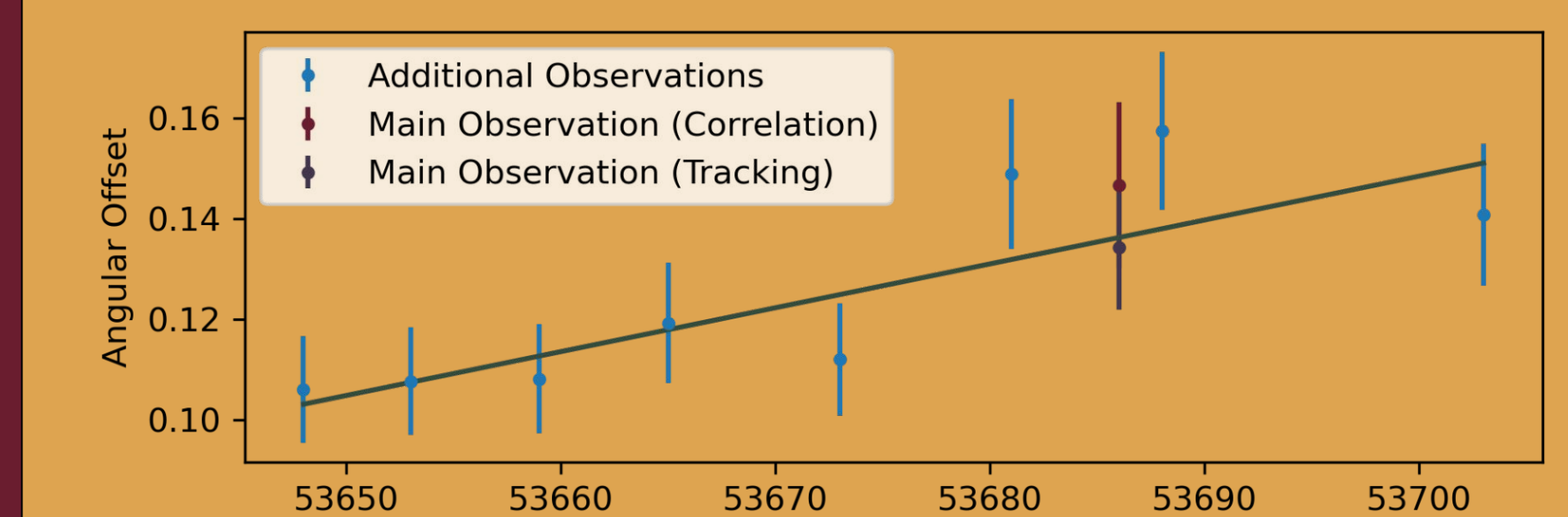


Figure 10: DM gradient induced angular offset over time. The green line corresponds to the best fit linear drift of $0.32 \pm 0.09 \text{ mas yr}^{-1}$

Ramifications

We have demonstrated how pulsar scintillation measurements can detect DM gradients on small scales by leveraging the multiple images formed by the screen, either by tracking single images over frequency or by looking for shifts of the arc as a whole. We find that a single measurement can determine the average gradient at the 10% level and that tracking over several observations leads to consistent results.

Unfortunately, the individual DMs of the observations were not measured so we cannot directly compare our gradient. However, we can compare to typical values from other systems. From the primary observation we get a temporal gradient of $6.7 \pm 0.8 \times 10^{-4} \text{ pc cm}^{-3} \text{ yr}^{-1}$, which compares very well with the values measured by Donner et al. 2020. Using LOFAR, they measured average values between 10^{-6} and 10^{-3} over the course of several years.